# Observed Variability in Soil Moisture in Engineered Urban Green Infrastructure Systems and Linkages to Ecosystem Services

**Bita Alizadehtazi[a], Patrick L. Gurian[a], and Franco A. Montalto[a,*]**

[a]Department of Civil, Architectural & Environmental Engineering, Drexel University, 3141 Chestnut Street, Philadelphia, PA 19104, USA

[*]Corresponding author: E-mail: fam26@drexel.edu

## Abstract

Soil-water-climate-vegetation interactions jointly determine the ability of landscapes to provide ecosystem functions and services. In particular, spatio-temporal patterns in soil moisture underpin landscape ecohydrology. Though these patterns have been of interest to researchers for some time, there is new interest in the topic today as city managers engineer green infrastructure (GI) into urban landscapes. This paper presents soil moisture data collected from 2012 to 2014, and weighing lysimeter observations continuing through 2016, in two urban GI systems. Relationships between precipitation history, season, soil depth, hydraulic loading ratio (HLR) on the frequency and magnitude of soil moisture responses are described quantitatively. A logistic regression model is used to quantify the odds that each of these variables triggers a detectable soil moisture response. The results suggest that the higher HLR site (Site 2, HLR = 3.8) had 129.7% higher odds of a soil moisture response than Site 1 (HLR = 1). The results also indicate that there are 82.9% lower odds of a response in summer than in winter. Moreover, the odds of a response decrease with increasing soil depth. The linkage between GI siting and design decisions that impact soil moisture and ecosystem services is illustrated by also reporting evapotranspiration (ET) rates at the sites as determined by the lysimeter. Higher ET observed during wetter conditions supports the hypothesis that GI siting and design factors that lead to higher moisture content can engender greater ecosystem services associated with this hydrologic process. Indeed, the higher HLR of Site 2 sustained higher soil moisture levels during the summer compared to Site 1.

**Keywords:** Urban soil moisture, Ecohydrology, Evapotranspiration, Hydraulic loading ratio, Ecosystem services

## 1. Introduction

Soil-water-climate and vegetation interactions jointly determine the ability of landscapes to provide a range of ecosystem functions and services (Costanza et al., 1997; MEA, 2005). Soil moisture, in particular, is directly related to photosynthesis (Galmés et al., 2007a; Pinheiro and Chaves, 2010), plant respiration (Burton et al., 1998; Galmés et al., 2007b), nutrient metabolism, gross and net primary productivity (Churkina and Running, 1998; Nemani et al., 2003; Ciais et al., 2005; Guo et al., 2016), biomass allocation (Comeau and Kimmins, 1989; Xu et al., 2010), surface vegetation cover and health (Adegoke and Carleton, 2002), carbon (Pastor and Post, 1986; Williams and Albertson, 2004; Kurc and Small, 2007) and nitrogen fluxes (Pastor and Post, 1986), as well as to the productivity-response patterns to rainfall pulses (Odum et al., 1995; Guo et al., 2016), and is thus a key determinant of landscape ecohydrology (Rodriguez-Iturbe, 2000). Though spatio-temporal patterns in soil moisture are, and have, been of keen interest to a wide range of researchers for some time (Famiglietti et al., 2008; Korres et al., 2010; Koyama et al., 2010; Rosenbaum et al., 2012; Korres et al., 2013; Vereecken et al., 2014; Dorigo et al., 2015; Korres et al., 2015; Huang et al., 2016), there is new interest in the topic today as city managers introduce nature-based solutions like engineered green infrastructure (GI) into the urban landscape (WWAP (United Nations World Water Assessment Programme), 2018).

In the last 1.5 decades, since GI was first proposed as an approach to urban stormwater management (NRDC, 2006), many researchers (Revelli and Porporato, 2018; Escobedo et al., 2019; Miller and Montalto, 2019) have espoused the wide range of ecosystem services (ES) that GI can provide. There is great interest in the ability of urban forests, distributed vegetated stormwater retention facilities (e.g. bioretention), and newly enhanced, restored, or created aquatic, riparian, and terrestrial habitats to intercept precipitation in the canopy, evapotranspire moisture from the soil, and otherwise regulate temperature (Susca et al., 2011), mitigate pollution of the air and water (Pugh et al., 2012; Jayasooriya et al., 2017), sequester carbon, and enhance human well-being (Bertram and Rehdanz, 2015; Rai et al., 2019). As GI implementation has proceeded, it has also become clear that GI can provide a range of ecosystem disservices (EDS)(Lyytimäki and Sipilä, 2009). For example, GI systems can attract vectors, pests, or pollen-producing vegetation.

Table 1, modified and adapted from Miller and Montalto (2019) is an attempt to summarize the role that soil moisture plays in determining the ability of GI to provide ecosystem functions and services/disservices, disaggregated by domain (e.g. air, soil, water, and human), and focusing on bioretention. Many of these services/disservices are dependent on vegetation, the health of which is determined by moisture availability. Soil moisture constrains the rate of evapotranspiration, modifying both water and energy balances (Petropoulos, 2013). The actual rate of ET modulates the partitioning of incoming radiation into latent and sensible heat, and the partitioning of incident precipitation into infiltration and runoff (Western et al., 1999).

This paper is part of a broader effort to study interactions between soil, water, climate, and vegetation in GI systems (DiGiovanni et al., 2012; Alizadehtazi et al., 2016; De Sousa et al., 2016a; De Sousa et al., 2016b; Smalls-Mantey, 2017; Alizadehtazi, 2018; DiGiovanni et al., 2018; Alizadehtazi et al., 2020). Here, we analyze several years of soil moisture data collected in two bioretention facilities that are similar in design and monitoring set up and that are located within two kilometers of one another. Specifically, we quantify the role of precipitation characteristics, season, and hydraulic loading ratio (the ratio of the tributary catchment area to the facility area, HLR) on soil moisture at different depths, making recommendations regarding specific GI siting and design decisions that can maximize provision of ecosystem services.

Table 1. Functions that potentially deliver ecosystem services and disservices through GI, and supporting role of soil moisture ([R] = regulating services; [S] = supporting services; [C] = cultural services)

| Domain | Description of potential function provided by green infrastructure | | Potential role of soil moisture in supporting function, direct or indirect | Potentially relevant in bioretention GI? |
|---|---|---|---|---|
| | Function leading to ecosystem service (ES) | Function leading to ecosystem disservice (EDS) | | |
| Air | Vegetation canopies influence the dispersion and promote deposition of airborne pollutants[1] (Air quality improvement[R]) | – | Supports plant growth | Yes |
| | Vegetation can reduce ambient air temperature through reflection (increased albedo), shading, or evapotranspiration[2] (Local climate regulation[R]) | – | Supports plant growth; source of water for evapotranspirative processes | Yes |
| | – | Vegetation is a source of pollen and can increase $O_3$ by releasing biogenic volatile organic compounds (BVOCs)[3] (Degrade air quality[R]) | Supports plant growth | Yes |
| | Vegetation and soil media attenuate sound waves[4] (Noise reduction[R]) | – | Supports plant growth; sound attenuation influenced by moisture state | Design dependent |
| Soil | Microbial activity enhances biogeochemical cycling (C and N) (Nutrient cycling[S]); Vegetation fixes carbon during photosynthesis, storing carbon as biomass fostering carbon storage and sequestration[5] (Climate regulation[R]) | – | Supports soil microbial communities and biomass; determines the redox state of the soil, affecting the stocks and direction of soil fluxes | Design dependent |
| | Vegetation and soil media capture, filter, sorb, retain and demobilize pollutants and nutrients originating in runoff[6] (Pollutant attenuation[R]) | Bioaccumulation of contaminants in soil (Pollutant attenuation[R]) | Supports plant growth; supports vegetation biomass, influencing the uptake of pollutants; determines pollutant solubility, redox state, and other biogeochemical processes related to phytoremediation | Yes |

Table 1. (continued)

| Domain | Description of potential function provided by green infrastructure: Function leading to ecosystem service (ES) | Description of potential function provided by green infrastructure: Function leading to ecosystem disservice (EDS) | Potential role of soil moisture in supporting function, direct or indirect | Potentially relevant in bioretention GI? |
|---|---|---|---|---|
| Soil | Vegetation and soil media provide habitat and support biodiversity[7] (Biodiversity restoration, habitat for invertebrates, birds, and wildlife[S]) | Vegetation and soil create new vectors and support nuisance insects and attract wildlife (e.g. wasps, mosquitoes, or rats); block views; may be perceived as unsafe during night-time; damage infrastructure by roots and microbial activity[8] (Social nuisances[C]) | Supports plants growth; enhances primary productivity | Yes |
| | Vegetation binds soil particles, retains and protects soil against wind and water, reducing sediment concentration load to water bodies[9] (Erosion control[R]) | Mobilization of sand, silt, and clay, increasing sediment loads to receiving water bodies (Soil erosion control[R]) | Support plant growths: soil moisture status determines mobilization and detachment of soil particles | Yes |
| Water | Vegetation intercepts and promotes the infiltration and detention of throughfall and runoff, increasing recharge, and decreasing water borne pollutant load through volume reduction[10] (Water regulation[R]) | – | Supports plant growth; direct determinant of saturated overland flow and Hortonian flow processes | Yes |
| Human | Vegetation and urban green spaces encourage positive social interactions and promote social cohesion; positive health behavior; enable stress reduction that enhances human well-being[11, C] | Vegetation is a source of pollen and can contribute to pollen allergy and asthma symptoms[12] (Impact human health and well-being[C]) | Supports plant growth | Yes |

[1](Litschke and Kuttler, 2008; Pugh et al., 2012)
[2](Taleghani, 2018)
[3](Chaparro and Terradas, 2009; Eisenman et al., 2019)
[4](Aylor, 1972; Van Renterghem and Botteldooren, 2011)
[5](Nowak and Crane, 2002; Kavehei et al., 2018; Kavehei et al., 2019)
[6](DiBlasi et al., 2009; LeFevre et al., 2015; Shrestha et al., 2018)

[7](Kazemi et al., 2009; Kazemi et al., 2011)
[8](Lyytimäki et al., 2008; Lyytimäki and Sipilä, 2009; Gómez-Baggethun and Barton, 2013)
[9](Maes et al., 2011; Liquete et al., 2015)
[10](Cook, 2007; Winston et al., 2016; Shrestha et al., 2018; Mahmoud et al., 2019)
[11](Hartig et al., 2003; Coutts and Hahn, 2015; Jennings and Bamkole, 2019)
[12](Eisenman et al., 2019)

## 2. Materials and methods

### 2.1. *Description of study sites and monitoring setups*

This research was conducted at two bioretention facilities located within two kilometers of one another in Queens, New York City (NYC). The two NYC sites were recently profiled as international examples of nature-based solutions to stormwater in WWAP (2018). The Colfax and Murdock Avenue bioretention facility (40.702, -73.743) (Site 1 in Fig. 1a) was built in 2010-11. This site receives only direct rainfall and is hydrologically isolated from surrounding impervious surfaces (HLR =1). The Nashville and 116th Street bioretention facility (40.698, -73.744) (Site 2 in Fig. 1b) was also built in 2010-11. This study focuses on a 125 $m^2$ vegetated space within it that receives street runoff through a curb cut as well as direct precipitation (HLR = 3.8). Both bioretention facilities were designed with similar vertical soil profiles, consisting of 60 cm of loamy sand on top of a thinner layer of crushed stone. The native soils underlying the facility were sandy and thus did not hinder infiltration. Some other physical properties of the site soils are shown in Table 2.

Extensive monitoring of the two sites has been conducted by the research team since the sites were initially constructed. This paper utilizes data gathered over five years (2012-2016) using the weighing lysimeter, climate stations, and soil moisture sensors installed at both sites. Technical specifications of these sensors are provided in Table 3. Data collected at each site was logged on a Campbell Scientific CR1000 data logger at 5-minute time intervals and transmitted via cell modem to a server for real time viewing.

The weighing lysimeters were custom designed as described in DiGiovanni (2013)(Fig. 2). All sensors were calibrated per the manufacturer's guidelines. The lysimeter weight was calibrated by applying fixed weights to the top of the soil column. The soil sensors were calibrated to the specific soil type used in the experiment.

Monitoring was conducted at two plots established at each site. The first plot was located inside the weighing lysimeter (termed “L”). The second was located outside the weighing lysimeter (termed “G”), but in a stand of vegetation similar to that found in the lysimeter (Figs. 3 and 4). Each plot was instrumented with five soil moisture sensors installed at 5, 10, 20, 30, and 50 cm depths in a circular pattern to avoid electrical interference between them. A specially designed flow diversion box and orifice ensures that the lysimeter at Site 2 is dosed with runoff at the same HLR as the rest of the site between mid-April and mid-October. During the colder winter months, the Site 2 lysimeter receives direct rainfall only. This seasonal shift in operation was necessary to avoid pipe rupture due to water expansion during freezing conditions. The lysimeter at Site 1 only receives direct precipitation.

The nomenclature used to refer to each sensor is a concatenation of the site number (1, 2), the plot location (L or G), and the soil sensor depth (5,10, 20, 30, 50). For example, the 1L5 refers to the lysimeter plot at Site 1, and specifically the soil sensor at 5 cm depth.

Both sites were planted with similar pallets of shrubs, and grasses immediately after construction. GI maintenance workers maintain the vegetation, replacing individual plants as needed. At the end of each growing season, the site maintenance protocol includes pruning and trimming. As shown in Figs. 3 and 4, at the beginning of each growing season, the vigor and canopy density inside and outside the lysimeters are similar. As the growing season progresses, the ground plots were typically covered by a more robust canopy coverage. Differences in canopy coverage then became smaller into the late autumn and winter, as plants naturally senesced and were manually pruned.


Fig. 1. Bioretention facilities: a) Colfax (Site 1), and b) Nashville (Site 2).

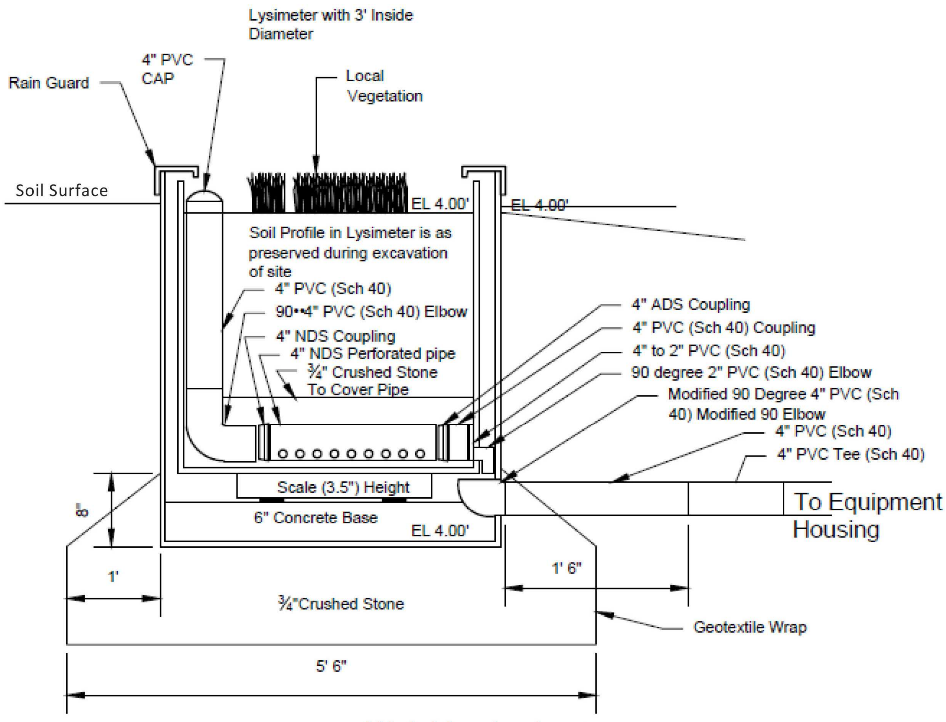


Fig. 2. Cross section of weighing lysimeter (not to scale).

Table 2. Physical properties of soils for Colfax (Site 1) and Nashville (Site 2) bioretention facilities (analysis performed by Golder Associates Inc., 6 years after facility installation)

| | | Colfax | Nashville |
|---|---|---|---|
| Soil classification | | USDA loamy sand | USDA loamy sand |
| Grain size | Sand | 82.2 % | 79.5 % |
| | Silt | 11.5 % | 12.6 % |
| | Clay | 6.3 % | 7.9 % |
| pH | | 7.6 | 7.7 |
| Organic content | | 2.5 | 2.3 |
| Porosity | | 39.4 % | 38.1 % |
| Specific gravity | | 2.61 g | 2.6 g |
| Bulk density | | 1486.5 kg $m^{-3}$ | 14302.5 kg $m^{-3}$ |
| Field capacity | | 0.18 $m^3/m^3$ | 0.22 $m^3/m^3$ |
| Wilting point | | 0.05 $m^3/m^3$ | 0.06 $m^3/m^3$ |

Table 3. Technical specifications of the equipment and sensors

| | Measured parameter | Equipment manufacture/model | Specifications | Installation height/depth |
|---|---|---|---|---|
| | Logger | Campbell Scientific, Inc. CR1000 | Logged at 5 min intervals | — |
| | Soil moisture/temperature | Decagon Devices 5TE Soil Sensor | Temperature: ±1°C<br>Soil moisture: ± 1-3% VWC | 5 cm<br>10 cm<br>20 cm<br>30 cm<br>50 cm |
| Climate station | Precipitation | Texas Electronics, Inc. Series 525 Rainfall Sensor | Up to 50 mm/h: ±1 % | 4 m height |
| | Wind speed and direction | Young Company Model 5103 | Wind speed: ±0.3 m/s<br>Wind direction: ±3° | 4 m height |
| | Long wave radiation (In/Out)<br>Shortwave radiation (In/Out) | Hukseflux Thermal Sensors NRO1 4-Compnemnt net-radiation sensor | ±10 % (Moderate quality, for daily sums) | 4 m height |
| | Air temperature and relative humidity | Campbell Scientific, Inc. CS215 | Air temperature: ±0.3 °C<br>Relative humidity: ±4% | 4 m height |
| | Evapotranspiration | Custom 0.657 $m^2$ Lysimeter | — | — |

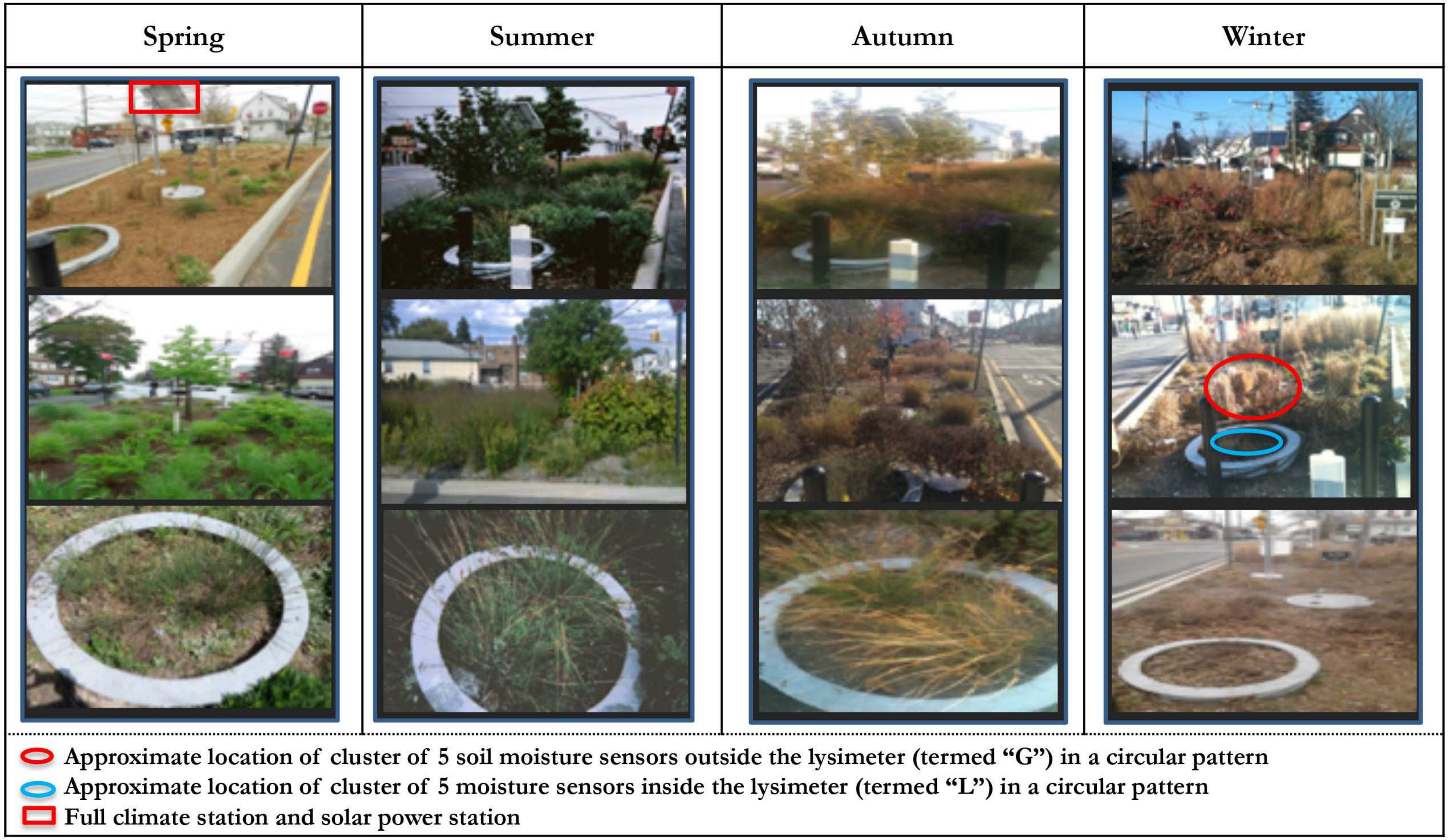


Fig 3. Seasonal canopy coverage at Site 1 inside the weighing lysimeter plot (L) and outside the weighing lysimeter plot (G). Also shown are the locations of the onsite weather station and soil moisture monitoring plots inside and outside the lysimeter.

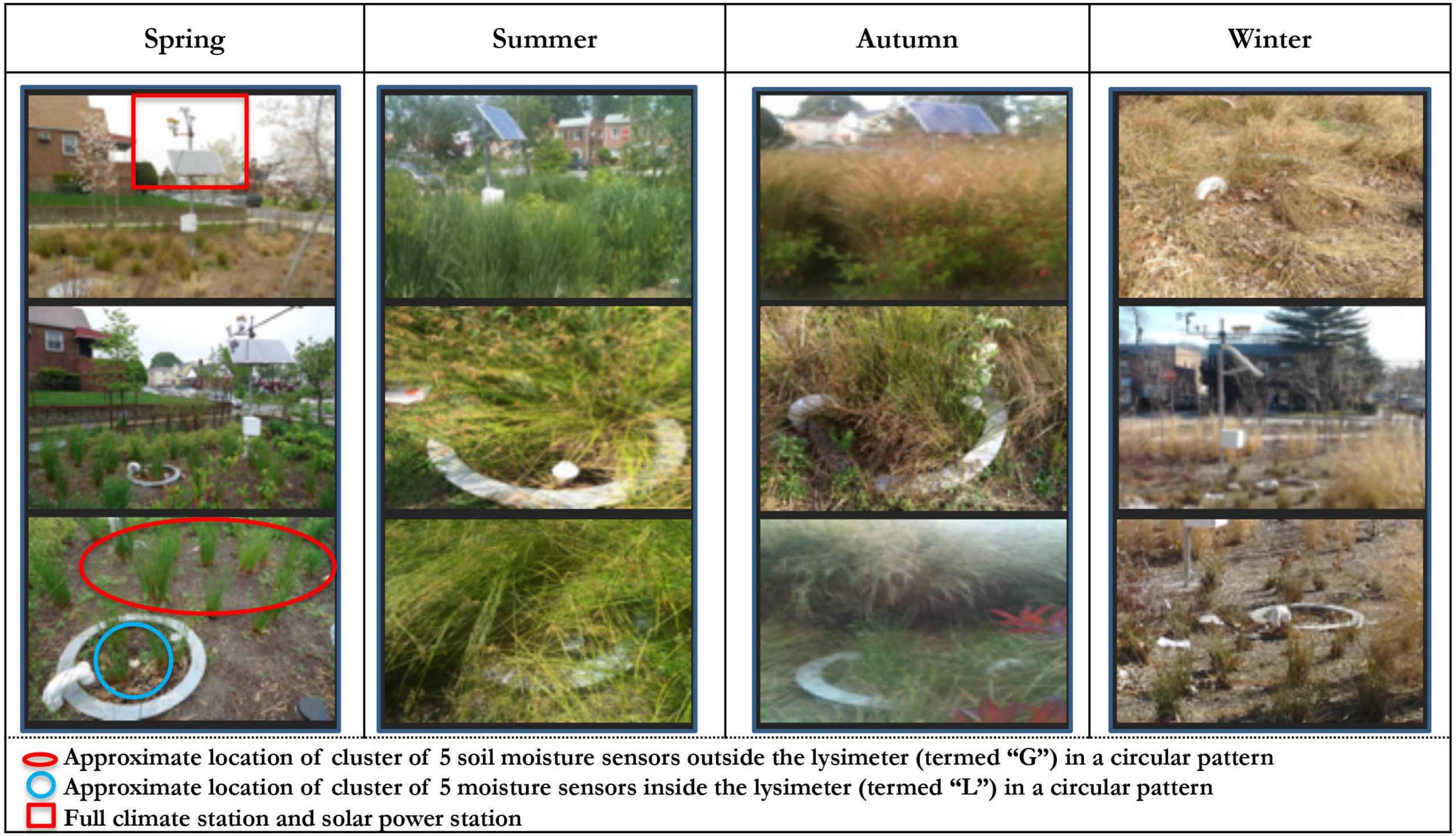


Fig 4. Seasonal canopy coverage at Site 2 inside the weighing lysimeter plot (L) and outside the weighing lysimeter plot (G). Also shown are the locations of the onsite weather station and soil moisture monitoring plots inside and outside the lysimeter.

## 2.2. ***Data processing and analysis***

Rainfall event separation

To evaluate spatial and temporal variability in soil moisture in response to precipitation, HLR, and season at the two sites the continuous precipitation time series needed to be discretized into individual events and analyzed. Precipitation had been logged at 5-minute intervals at each site using the precipitation gages (Table 3). Individual events between 2012 and 2014 were defined using a four-hour inter-event dry period, following prior convention (Yu et al., 2018; Yu et al., 2019). The resulting events were then further categorized into seven different depth bins (0-2, 2-5, 5-10, 10-15, 15-20, 20-30, 30-140 mm). Extreme events were defined as events that exceeded 30 mm per event, also following prior convention (De Sousa et al., 2016a).

Difference in soil moisture

For reference, the full soil moisture time series data collected at both locations at each of the two sites during 2012-2014 are presented in Alizadehtazi and Montalto (2020). Here, the frequency and the magnitude of the soil moisture responses embedded in the time series are presented on an event basis. The soil moisture response frequency was defined on a seasonal basis as the fraction of all precipitation events demonstrating a significant (e.g. at least a 5%) change over the pre-storm value. To quantify changes in soil moisture over each rain event, the magnitude of the response was computed as $\left\{\frac{(\theta m-\theta i)}{\theta i}\right\} \times 100$, where $\theta_m$ is defined as the maximum volumetric moisture content observed during the event, and $\theta_i$ is the pre-storm volumetric moisture content.

Seasonal changes in soil moisture

Seasonal changes in soil moisture were evaluated using the lysimeter weight differences. Although soil moisture data was only available for three years (2012-2014), climate and weighing lysimeter observations were made over a longer period (2012-2016). Increases in weight were associated with soil wetting, while decreases in weight were associated with soil drying.

Actual and Reference ET calculations

The changes in lysimeter weight were also used to compute actual evapotranspiration (AET) at the two sites as follows:

$$AET = \sum_{i=1}^{12} \left( f \frac{m_i - m_{i+1}}{A\rho_w} \right)_i \qquad (1)$$

where, AET is the evapotranspiration (mm h$^{-1}$), $m_i$ and $m_{i+1}$ are the weights of the lysimeter at consecutive hourly sampling intervals (kg), $A$ is the surface area of the lysimeter (0.657 m$^2$), $\rho_w$ is the density of water assumed constant at 1000 kg m$^{-3}$, and $f$ is a conversion factor equal to 1000 (mm m$^{-1}$). No AET values were computed within 48 hours of rain events to avoid potential errors associated with percolation-related weight changes, following standard practice (Jensen and Allen, 2016). Negative AET values (e.g. weight increases) were attributed to precipitation and condensation.

To contextualize the AET values, the American Society of Civil Engineers (ASCE) Standardized Reference Evapotranspiration (RET) Equation (ASCE, 2005) was used to compute RET using onsite climate data logged with the climate station (Table 3):

$$RET = \frac{0.408\Delta(R_n - G) + \gamma \frac{C_n}{T + 273} + u_2(e_s - e_a)}{[\Delta + \gamma(1 + C_d u_2)]} \quad (2)$$

where:

RET = standardized reference ET (mm $h^{-1}$)

$\Delta$ = slope of saturation vapor pressure-temperature curve (kPa °$C^{-1}$)

$R_n$ = calculated net radiation at the crop surface (MJ $m^{-2}$ $h^{-1}$)

$G$ = heat flux density at the soil surface (MJ $m^{-2}$ $h^{-1}$)

$\gamma$ = psychrometric constant (kPa °$C^{-1}$)

$C_n$= numerator constant that changes with reference surface and calculation time step, 37 for short (grass) reference surface at hourly time step (K mm $s^3$ $Mg^{-1}$ $h^{-1}$)

$T$ = mean hourly air temperature at 1.5 to 2.5 m height (°C)

$u_2$ = hourly wind speed at 2-m height (m $s^{-1}$)

$e_s$ = mean saturation vapor pressure (kPa)

$e_a$ = mean actual vapor pressure (kPa)

$e_s - e_a$= vapor pressure deficit (kPa)

$C_d$ = denominator constant that changes with reference type and calculation time step (s $m^{-1}$)

Because RET represents an upper bound to AET for the local microclimate, soil moisture is assumed to be constraining ET, and the ecosystem services linked to it whenever AET < RET.

Logistic regression model

A binary logistic regression (Peng et al., 2002; Hosmer et al., 2013) was developed in

RStudio version 1.0.44 (RStudio Team, 2016) running R version 3.3.2 (R Core Team, 2016) to analyze the effect of certain independent variables (e.g. site, location, season, soil depth, and rainfall depth bin) on the soil moisture response to precipitation. The model was used to predict the dependent variable, (e.g. the occurrence of a response), from the set of predictor variables. The soil moisture response was coded as "1" if there was a response, and "0" if there was no response. The regression model predicts the natural log of the odds ratio (OR) for a response versus no response categorical outcome. A positive regression coefficient (β) indicates an increase in the odds of a response. The model was trained on 80% of the data and tested on the remaining 20% of the data. Receiver Operating Characteristic (ROC) curve was used to evaluate the overall predictive capability of the logistic model. Accuracy was measured by the area under the ROC curve (AUROC), with an area of 1.00 representing a perfect fit and 0.50 indicating the model is no better than random guessing.

## 3. Results

### 3.1. *Onsite monitored precipitation*

Figure 5a shows the total cumulative depth of seasonal precipitation (e.g. summed over 5 years) at Sites 1 and 2. The seasonal trends were similar between the two sites with cumulative summer totals slightly higher than the other seasons. The 2012 to 2014 precipitation only was used to separate events in order to analyze vertical differences in soil moisture. A total of 151 events were defined from the 5-minute data collected during those periods, with similar distributions observed at the two sites (Fig. 5b).

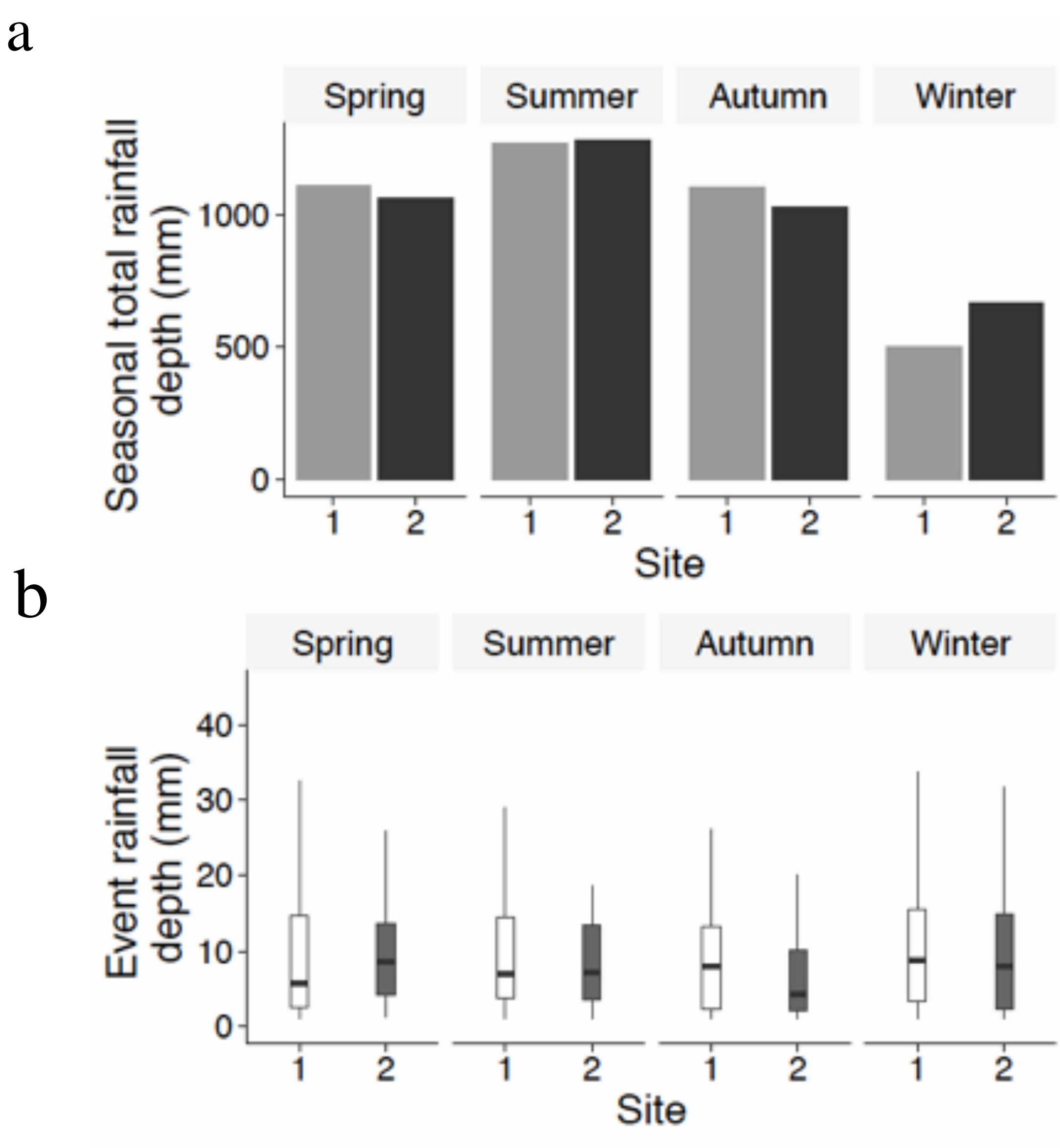


Fig. 5. The seasonal precipitation quantities measured at Site 1 and Site 2 from 2012 to 2016, and b) discrete event rainfall depth from the continuous rainfall record during 2012-2014 using a four-hour inter-event dry period (outliers not shown). NOTE: The middle part of the box plot is interquartile range (IQR: distance between the third and first quartiles). The line near the middle of the box represents the median. The lower and upper hinges correspond to the first and third quartiles (the 25$^{th}$ and 75$^{th}$ percentiles: values below which percentage of data fall). The upper whisker extends from the hinge to the largest value no further than 1.5 * IQR from the hinge. The lower whisker extends from the hinge to the smallest value at most 1.5 * IQR of the hinge.

### 3.2. ***Spatial differences in soil moisture***

The 100% stacked bar plots in Fig. 6 display the seasonal frequency of soil moisture responses to all precipitation events at Site 1 and Site 2 (Fig. 6a). In Fig. 6b the seasonal response frequencies were further broken down by location (L vs. G) at Site 1 (left) and Site 2 (right).

As a function of site

In general, a greater frequency of a response was observed at Site 2 than at Site 1 across all seasons (except for in winter, when similar values were observed at both sites) (Fig. 6a).

As a function of location

The frequency of soil moisture response observed in the ground plots was lower than in the lysimeter plots at both sites (Fig. 6b). Comparing just the lysimeter plots and focusing only on spring and summer when 2L receives offsite runoff, the average frequency of soil moisture response at Site 1 was 53.5%, whereas at Site 2 it was 80%. The same general trend was observed for all seasons in the ground plots, e.g. 39.5% at Site 1 and 52.8% at Site 2.

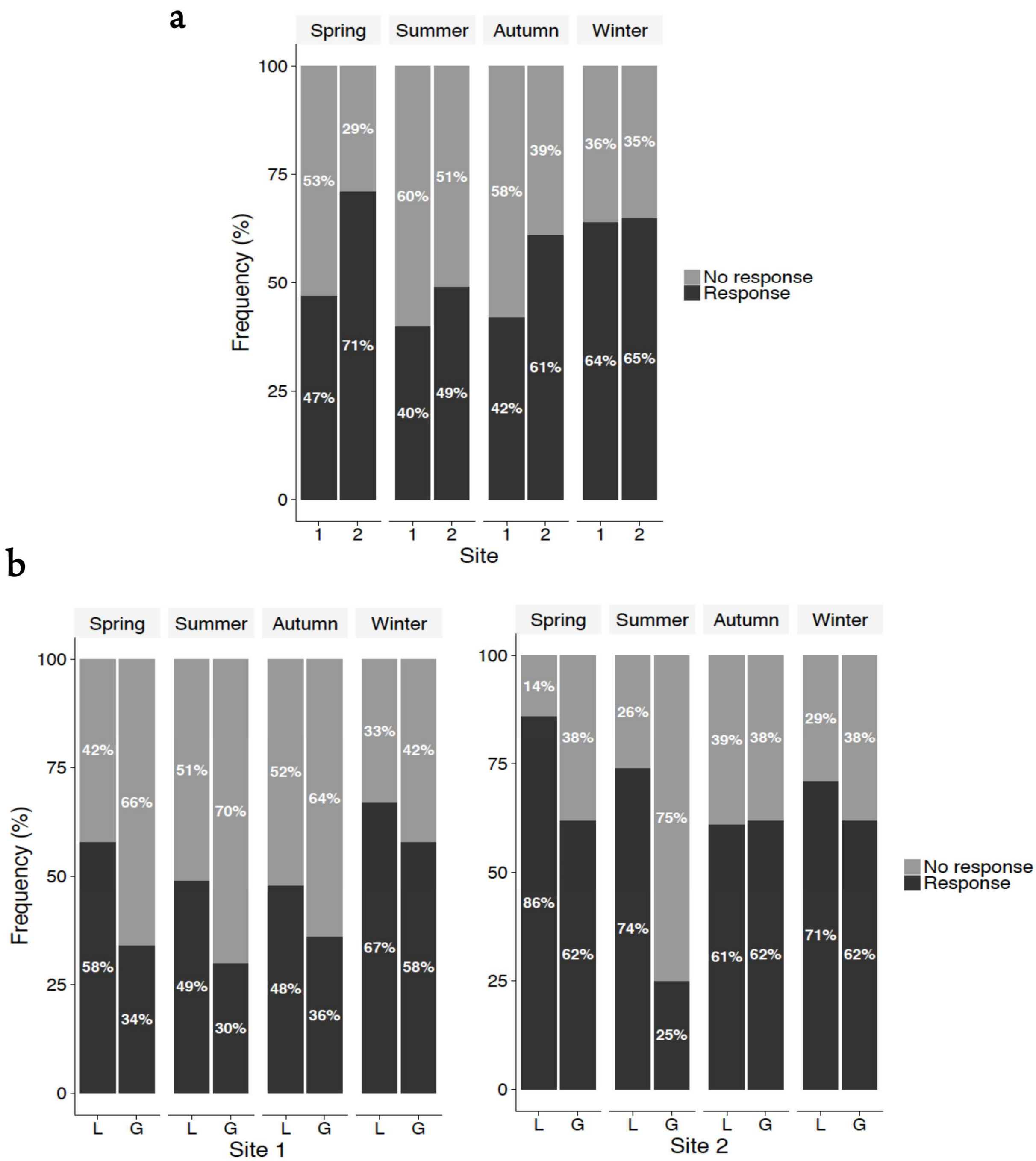


308

309 Fig. 6. The seasonal frequency of a response: (a) as a function of Site (Site 1 vs. Site 2), (b) as a
310 function of location (L vs. G) at Site 1 (left), at Site 2 (right).

### 3.3. ***Vertical differences in soil moisture***

The magnitude and frequency of the observed soil moisture responses to all precipitation events are presented in Table 4 for the two monitoring locations at Site 1, and in Table 5 for the two monitoring locations at Site 2. While Fig. 6b reported the frequency of a response to all events at any depth at both locations at each site, Tables 4 and 5 further subdivides the observations by soil depth (5, 10, 20, and 30, and 50 cm). Because all the sensors at any given location were not always working at the same time, there are slight differences in the number of events ("*Event N"*) analyzed at each depth. The range in the magnitude of the responses at each depth is presented as a box plot, while the frequency of a response is presented as a bar plot.

<u>As a function of soil depth</u>

With very few exceptions, the frequency of the soil moisture response was reduced with depth. The frequency generally varied from an average of 70% at the 5 cm depth to an average of 24% at the 50 cm depth, with a few anomalies: 1L30 in autumn, 1G20 in summer and autumn, 1G30 in spring and summer, and 2L30 in summer and autumn, which showed increases of between 2 and 18% in the frequency of a response compared to the next highest sensor. In general, the magnitude of the soil moisture response was also dampened with depth, though this trend was much more pronounced at Site 1 (both locations) than at Site 2.

Table 4. Site 1 seasonal frequency[a] and magnitude[b] of a soil moisture response for five different soil depths (5, 10, 20, 30, and 50 cm) inside (L) and outside the lysimeter plots (G)

| | Spring | | | Summer | | | Autumn | | | Winter | | |
|---|---|---|---|---|---|---|---|---|---|---|---|---|
| Plot ID | Magnitude % | Event N | Frequency % | Magnitude % | Event N | Frequency % | Magnitude % | Event N | Frequency % | Magnitude % | Event N | Frequency % |
| | 0 50 100 150 | | 0 50 100 | 0 50 100 150 200 | | 0 50 100 | 0 50 100 150 200 | | 0 50 100 | 0 50 100 150 | | 0 50 100 |
| 1L5 | | 43 | | | 37 | | | 30 | | | 41 | |
| 1L10 | | 43 | | | 37 | | | 33 | | | 41 | |
| 1L20 | | 43 | | | 37 | | | 33 | | | 41 | |
| 1L30 | | 43 | | | 37 | | | 33 | | | 41 | |
| 1L50 | | 43 | | | 37 | | | 33 | | | 41 | |
| | 0 50 100 150 | | 0 50 100 | 0 50 100 150 | | 0 50 100 | 0 50 100 150 | | 0 50 100 | 0 50 100 150 | | 0 50 100 |
| 1G5 | | 36 | | | 34 | | | 33 | | | 24 | |
| 1G10 | | 36 | | | 34 | | | 33 | | | 24 | |
| 1G20 | | 36 | | | 34 | | | 33 | | | 24 | |
| 1G30 | | 36 | | | 34 | | | 33 | | | 24 | |
| 1G50 | | 36 | | | 34 | | | 33 | | | 24 | |

[a] Defined on a seasonal basis as the fraction of all precipitation events demonstrating at least a 5% change over the pre-storm value.

[b] Computed as $\left\{\frac{(\theta m-\theta i)}{\theta i}\right\} \times 100$, where $\theta_m$ is the maximum moisture content observed during the event, and $\theta_i$ is the pre-storm value.

Table 5. Site 2 seasonal frequency[a] (See Table 4) and magnitude[b] (See Table 4) of a soil moisture response for five different soil depths (5, 10, 20, 30, and 50 cm) inside (L) and outside the lysimeter plots (G)

| | Spring | | | Summer | | | Autumn | | | Winter | | |
|---|---|---|---|---|---|---|---|---|---|---|---|---|
| Plot ID | Magnitude % | Event N | Frequency % | Magnitude % | Event N | Frequency % | Magnitude % | Event N | Frequency % | Magnitude % | Event N | Frequency % |
| | 0 50 100 150 200 250 | | 0 50 100 | 0 50 100 150 200 | | 0 50 100 | 0 100 200 300 400 500 | | 0 50 100 | 0 50 100 150 | | 0 50 100 |
| 2L5 | | 17 | | | 16 | | | 15 | | | 26 | |
| 2L10 | | 17 | | | 15 | | | 15 | | | 26 | |
| 2L20 | | NA | | | NA | | | 11 | | | NA | |
| 2L30 | | 17 | | | 16 | | | 15 | | | 26 | |
| 2L50 | | NA | | | NA | | | NA | | | NA | |
| | 0 50 100 150 200 | | 0 50 100 | 0 50 100 150 200 | | 0 50 100 | 0 50 100 150 | | 0 50 100 | 0 50 100 150 | | 0 50 100 |
| 2G5 | | 17 | | | 10 | | | 7 | | | 26 | |
| 2G10 | | 17 | | | 10 | | | 7 | | | 26 | |
| 2G20 | | 17 | | | 10 | | | 7 | | | 26 | |
| 2G30 | | 17 | | | 10 | | | 7 | | | 26 | |
| 2G50 | | 17 | | | 8 | | | 6 | | | 26 | |

### 3.4. ***Precipitation-driven differences in soil moisture***

The level plots in Fig. 7 display the soil moisture response frequency over the 151 individual events, binned by precipitation event depth (0-2, 2-5, 5-10, 10-15, 15-20, 20-30, 30-140 mm). For simplification, only the results at 5 and 50 cm depths are shown. The frequencies for 1L5 and 1L50 are shown in Fig. 7a, 1G5 and 1G50 in Fig. 7b, 2L5 and 2L50 in Fig. 7c, and 2G5 and 2G50 in Fig. 7d. Separate columns are provided for each season. The lighter colored regions represent less frequent responses, while the darker regions denote more frequent responses, and light grey regions denote missing data. The numbers in each of the boxes indicate the number of rainfall events that were associated with each site, location, depth, and season combination.

<u>As a function of precipitation depth</u>

In general, across both sites, both locations, and all seasons, the frequency of a soil moisture response to precipitation was greater at the 5 cm depth, than at the 50 cm depth. Larger precipitation events were also generally associated with more frequent soil moisture responses. Extreme precipitation events (> 30 mm) nearly always triggered a response at 5 cm depth, except for 2G5 during the summer.

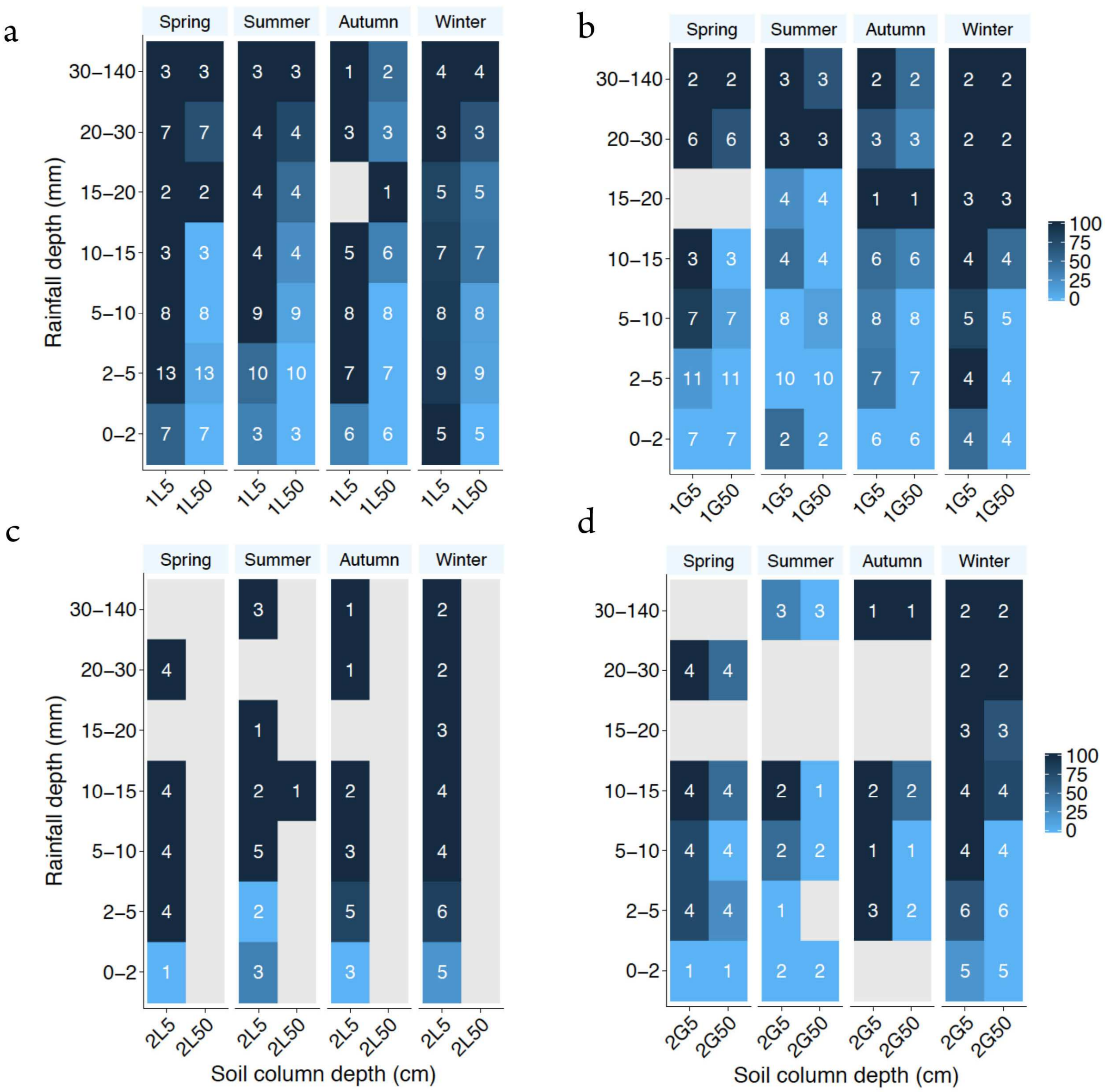


Fig. 7. Seasonal frequency of a soil moisture response to rainfall pulses. Level plots are provides for 5 and 50 cm depths only: a) Site 1 inside the lysimeter plot (1L5 and 1L50), b) Site 1 outside the lysimeter plot (1G5 and 1G50), c) Site 2 inside the lysimeter plot (2L5 and 2L50), and d) Site 2 outside the lysimeter plot (2G5 and 2G50).

### 3.5. ***Seasonal differences in soil moisture***

Seasonal differences in soil moisture response were evident in the data presented in Figs. 6-7 and Tables 4-5. Generally, at Site 1, which receive no offsite runoff, the winter brought the most frequent, and summer the least frequent, soil moisture responses. This observation was repeated regardless of location, soil depth, and precipitation event. Focusing only on the ground plots at both sites (to avoid differences in response due to solely to operation of the lysimeter), soil moisture responses were found to be most frequent in winter (Site 1 = 58%, Site 2 = 62%) and least frequent in summer (Site 1 = 30%, Site 2 = 25%) (Fig. 6b). In general, the spring and autumn frequency responses were of intermediate frequencies.

Moreover, the data presented in Tables 4-5 revealed higher winter frequencies at all soil depths of the ground plots at both sites (with 2G5 and 2G30 in spring, and 2G5 in autumn as exceptions). This same trend (winter frequency > summer frequency) was true for nearly all non-extreme precipitation event depths recorded at both ground plots (Fig. 7b and 7d). The magnitude of the soil moisture response in the ground plots is also greater during the winter than in the summer, for all soil depths (Tables 4-5).

Nearly identical trends in the frequency and magnitude of soil moisture response were observed at 1L, the only site that has consistent operation over the year. The seasonal response frequency decreased through the year, from 67% in winter, to 58% in spring, to 49% in summer, to 48% in autumn (Fig. 6b – left). Table 4 indicates that the winter soil moisture response frequencies were greater than summer at all soil depths, and Fig. 7a shows this same trend to be true for all small precipitation events (e.g. < 5 mm). An accurate comparison of the winter and summer response frequencies at Site 2L was not possible due to seasonal differences in Site 2 lysimeter operation as described above.

The observed seasonal differences in soil moisture response mirrored trends in seasonal soil wetness, as inferred from the lysimeter weight values. Figure 8a and 8b display the monthly lysimeter weight, as recorded during 2012 -2016 at Site 1 and Site 2, respectively. A direct measurement of the total quantity of moisture stored in the entire soil column, the lysimeter weight generally decreased from winter through spring and into summer, increased again in the autumn. This seasonal trend was more pronounced at Site 1 than at Site 2, and particularly intriguing given that summer precipitation at both sites exceeded the other seasons (Fig. 5a).

### 3.6. ***Seasonal differences in evapotranspiration***

Figure 8c and 8d depict monthly actual and reference evapotranspiration between 2012 and 2016. The monthly trend in RET was nearly the inverse of the trend in lysimeter weight. That is, RET was highest when the lysimeter weight was lowest. RET values were lowest in the winter, began to rise in the spring, peaked in summer, and then began to drop again in the autumn, the exact inverse of the lysimeter weight trend. The trend in AET values was similar, but with AET values slightly lower than RET values, as expected. The RET values at both sites were similar which is not unexpected given their physical proximity to one another.

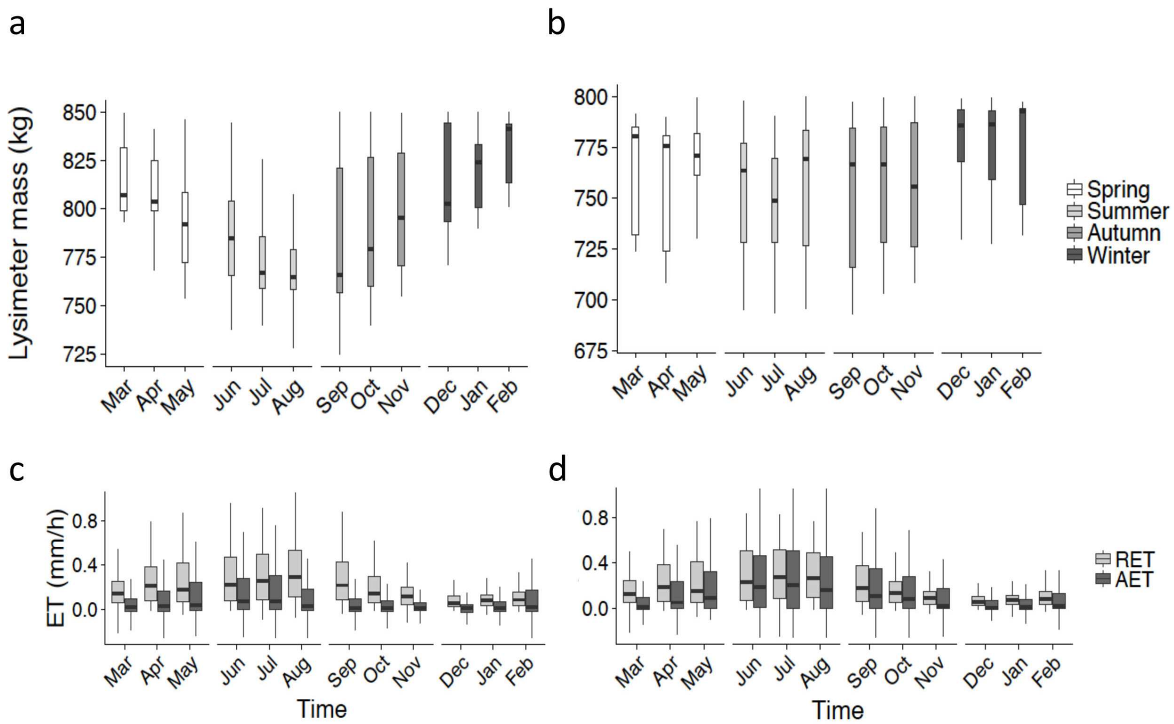


Fig. 8. The monthly aggregate soil moisture and evapotranspiration during 2012 -2016: a) Site 1 monthly lysimeter mass, b) Site 2 monthly lysimeter mass, c) Site 1 monthly AET and RET, and d) Site 2 monthly AET and RET (outliers not shown). NOTE: a description on the box plot anatomy is provided in Fig. 5 caption.

## 4. Discussion

To discuss these results quantitatively, a logistic regression model was developed to explore the roles of various predictor variables on the observed soil moisture responses. The results, presented in Table 6, indicate that all predictor variables (site, location, season, soil depth, and rainfall depth bin) were significantly correlated to the odds of a soil moisture response. The model demonstrated a reasonable fit, with 84.9% accuracy and AUROC = 0.92.

The odds ratio, exp (β), for the variable "location" indicated that ground plots had 72% lower odds of showing a soil moisture response than the lysimeter plots. The lower frequency of soil moisture response observed in the ground plots relative to the lysimeter plots (Fig. 6b) could be attributed to lesser late summer canopy coverage in the lysimeter, as described in the Methods and shown visually in Figs. 3 and 4. The more robust canopy that developed over the growing season above the ground plots could have attenuated a portion of the incident rainfall, limiting infiltration and associated soil moisture increases near the sensors. Though the vegetation inside the lysimeters also became more robust over the growing season, the lysimeter soil surfaces were more exposed to precipitation than the ground plots, creating more opportunities for infiltration and associated soil moisture responses.

The odds ratio for the variable "Site" indicated that Site 2 had 129.7% higher odds of showing a response than Site 1. This result could be indicative of the higher HLR of Site 2 and its receipt of offsite runoff from adjacent impervious surfaces through the curbcut inlet. In addition to incident precipitation, this additional inflow may explain the higher overall frequency and magnitude of soil moisture responses at Site 2 (Fig. 6 and Tables 4 and 5). The greater HLR increased the site's overall moisture state.

Table 6. Binary logistic regression model results with predictive variables such as site, location, season, soil depth, and rainfall depth bin

| Variables in the equation | β | Sig.[a] | Exp(β) |
|---|---|---|---|
| Site | | | |
| Site 1 | reference | reference | reference |
| Site 2 | 0.832 | *** | 2.297 |
| Location | | | |
| Ground | reference | reference | reference |
| Lysimeter | 1.276 | *** | 3.584 |
| Season | | | |
| Winter | reference | reference | reference |
| Spring | -0.547 | ** | 0.579 |
| Summer | -1.767 | *** | 0.171 |
| Autumn | -1.005 | *** | 0.366 |
| Soil depth | | | |
| 5 cm | reference | reference | reference |
| 10 cm | -1.195 | *** | 0.303 |
| 20 cm | -1.473 | *** | 0.229 |
| 30 cm | -2.143 | *** | 0.117 |
| 50 cm | -3.860 | *** | 0.021 |
| Rainfall depth bin | | | |
| 0-2 | reference | reference | reference |
| 2-5 | 1.643 | *** | 5.170 |
| 5-10 | 3.045 | *** | 21.009 |
| 10-15 | 4.588 | *** | 98.336 |
| 15-20 | 5.157 | *** | 173.583 |
| 20-30 | 6.475 | *** | 648.906 |
| 30-140 | 6.106 | *** | 448.406 |

[a]Sig. codes: *** = 0, ** = 0.001

The odds ratio for the variable "season" indicated that there were 82.9% lower odds of a response in summer than in winter. This finding was not surprising given the greater canopy coverage and associated interception in summer. Spring had 42.1% lower odds than winter potentially for the same reason.

Soil depth had a negative effect on the odds of a response. In other words, the odds of a response decreased with increasing soil depth. For example, at 10 cm depth there was a 69.7% lower odds of a response than at 5 cm depth, while at 50 cm depth there was a 97.9% lower odds than at 5 cm. This result is not surprising since infiltrating water fills the upper unsaturated soil pores first, with percolation to lower pore spaces occurring only if the volume of infiltrating water exceeds the available pore space.

Variability in soil moisture was more common in the upper soils than in the lower soils, and the magnitude of the response in the upper soil was also greater (Tables 4 and 5). Other researchers have also found that precipitation triggered more frequent responses closer to the surface (Yao et al., 2013) and reported decreasing soil moisture with increasing depth (Penna et al., 2013). This observation suggests that ecosystem services that require alternating wet/anaerobic and dry/aerobic conditions, such as nitrification/denitrification, biodegradation of hydrocarbons (Groffman and Tiedje, 1989; Maag and Vinther, 1996; Pihlatie et al., 2004; Burgin and Groffman, 2012), may be more likely to occur in the upper soil than in the lower soils of urban green spaces. The corollary is that ecosystem services that are more prevalent under steady soil moisture/redox conditions, may be more likely to occur at greater depths in GI systems.

Hydraulic loading seems to play a role in increasing the soil moisture response in the upper soils, especially inside the lysimeter, and especially during the growing season. The greater HLR reduced the variability of the site's moisture regime, perhaps favoring ecosystem services associated with less variable moisture/redox state. From an ecohydrological standpoint, the higher and more stable moisture state means that AET more closely approaches the reference rate established by local climatic conditions. As plants transpire more, they also perform more photosynthesis. The deliberate redirection of urban runoff toward urban green spaces thus seems like it can enhance the water regulation, climate regulation, and supporting services achievable in urban GI.

The rainfall depth bin variable had a positive effect on the odds ratio of a soil moisture response, and it increased from each rainfall depth bin to the next bin. At both HLR's investigated here, larger precipitation events triggered more frequent soil moisture responses, suggesting a feedback loop. It appears that patterns of precipitation and runoff determine the soil moisture patterns, which in turn, could establish soil biogeochemical conditions that better support biota. With other climatic factors, it is the biota and the soil moisture state of the soil that determine the rate of actual evapotranspiration, producing a localized effect on the microclimate. Small precipitation events are much more frequent than larger events in the temperate climate in which this research was conducted. However, the predicted increase in the frequency of larger precipitation events (NPCC, 2013) can thus be expected to trigger more frequent soil wetting, with associated impacts on all of the ecohydrologic and biogeochemical processes that are driven by it. It is especially significant that nearly all the extreme precipitation events that occurred during this study period triggered a soil moisture response even at 50 cm below the surface.

Perhaps the most intriguing set of observations was that the frequency of a soil moisture response was directly proportional to the moisture content of the soil, and inversely proportional to AET (Fig. 8). Vegetation-mediated ET depleted soil moisture in the warmer months and allowed it to build during the cooler months. Indeed, it appears that the higher HLR allowed site 2 to stay wetter, and to evapotranspire more water, during the peak growing seasons. The higher moisture and accelerated ET likely enhance the regulating services provided by Site 2, including water regulation (e.g. as influenced by evapotranspirative fluxes) and climate regulation, since ET is a temperature neutral phase change process. At higher moisture contents, there was less available pore space for infiltrating precipitation to occupy, triggering a more frequent, deeper, and more significant soil moisture response to precipitation. Though not measured explicitly here, it is likely that the opportunity for runoff and recharge are also greater in the winter months (e.g. saturation excess). Precipitation applied to wet winter soils may also displace antecedent soil moisture downward, while ponding and potentially running off when pore space capacity is completely depleted. Additional work would ideally compare how all of these factors (climate, hydraulic loading, and vegetation) impact these two environmentally significant processes, tied to the water regulating ecosystem service provided by urban green spaces.

## 5. Conclusions

This study presented observed relationships between the frequency and magnitude of soil moisture responses of engineered GI systems to precipitation, season, soil depth, and HLR, and discussed the potential significance of these responses to the soil-water-climate-vegetation dynamics that underpin GI's relationship to some ecosystem services and disservices. Variability of soil moisture was more common in the upper soils than in the deeper soils and the magnitude of the response was also greater in the upper soils. Indeed, the routing of offsite runoff to Site 2 increased the frequency of its soil moisture response and increased the depth to which a response was detected. The greater HLR reduced the variability of the site's moisture regime, a phenomenon that could promote ecosystem services associated with less variable moisture/redox state. The higher moisture state allowed the Site 2 to evapotranspire closer to the local reference rate, as established by local climatic conditions. Redirection of urban runoff to green spaces potentially maximizes the water regulation, climate regulation, and supporting services and disservices provided by urban GI.

To our knowledge, the potential ecohydrologic significance of seemingly mundane decisions regarding the siting of GI systems on an urban street have not previously been reported. Although the soil moisture patterns observed in GI systems that do, and do not, receive offsite runoff differ significantly from one another, it is only through a watershed scale investigation that GI's potential for delivering urban ecosystem services can be fully quantified. An upscaled analysis would need to take into consideration the maximum buildout of green spaces within the watershed, and their designed hydraulic connections to adjacent impervious tributary drainage areas.

As pointed out in WWAP (2018), nature-based solutions have maximum impact when protocols governing their design and management are customized to local conditions and context. Ideally, this study would be replicated at other locations with different underlying geology, soils, microclimates, vegetation types, and hydrologic loading rates. Such field monitoring is challenging in urban settings due to logistic issues associated with monitoring system power and data transmission requirements, as well as vandalism. Additional research would ideally also include laboratory studies to test the role of vegetation canopies on infiltration, recharge, and runoff processes, as well as catchment modeling to better understand the potential role that engineering decisions associated with application of runoff to urban green spaces and anthropogenic climate change may have on soil biogeochemistry and the ecosystem services dependent on it.

**Acknowledgements**

This research was partially funded by the National Science Foundation through *CAREER: Integrated Assessments of the Impacts of Decentralized Land Use and Water Management* (CBET: 1150994), and *Coastal SEES (Track 2), Collaborative: Developing High Performance Green Infrastructure Systems to Sustain Coastal Cities* (CMMI: 1325328), and the National Oceanic and Atmospheric Association (NOAA) through *Supporting Regional Implementation of Integrated Climate Resilience: Consortium for Climate Risks in the Urban Northeast (CCRUN) Phase II* (NA15OAR4310147). The authors acknowledge contributions to this paper by Lauren Smalls-Mantey, Kimberly DiGiovanni, and Leena Shevade.

**References**

Adegoke, J.O., Carleton, A.M., 2002. Relations between soil moisture and satellite vegetation indices in the US Corn Belt. Journal of Hydrometeorology, 3(4): 395-405.

Alizadehtazi, B., 2018. The evolution and significance of soil, soil Surface, and soil moisture in the ecohydrology of engineered urban green spaces., Doctoral dissertation.Drexel University, Philadelphia, PA.

Alizadehtazi, B., DiGiovanni, K., Foti, R., Morin, T., Shetty, N.H., Montalto, F.A., Gurian, P.L., 2016. Comparison of observed infiltration rates of different permeable urban surfaces using a cornell sprinkle infiltrometer. J. Hydrol. Eng., 21(7): 06016003. DOI:https://doi.org/10.1061/(ASCE)HE.1943-5584.0001374

Alizadehtazi, B., Gurian, P.L., Montalto, F.A., 2020. Impact of successive rainfall events on the dynamic relationship between vegetation canopies, infiltration, and recharge in engineered urban green infrastructure systems. Ecohydrology, 13(2): e2185.

Alizadehtazi, B., Montalto, F.A., 2020. Precipitation and soil moisture data in two engineered urban green infrastructure facilities in New York City. Data in brief.

ASCE, 2005. The ASCE Standardized Reference Evapotranspiration Equation. Report of the Task Committee on Standardization of Reference Evapotranspiration. Environmental and Water Resources Institute (EWRI) of the American Society of Civil Engineers (ASCE), Reston, VA, USA.

Aylor, D., 1972. Noise reduction by vegetation and ground. The Journal of the Acoustical Society of America, 51(1B): 197-205.

Bertram, C., Rehdanz, K., 2015. The role of urban green space for human well-being. Ecological Economics, 120: 139-152.

Burgin, A.J., Groffman, P.M., 2012. Soil O2 controls denitrification rates and N2O yield in a riparian wetland. Journal of Geophysical Research: Biogeosciences, 117(G1).

Burton, A.J., Pregitzer, K.S., Zogg, G.P., Zak, D.R., 1998. Drought reduces root respiration in sugar maple forests. Ecological Applications, 8(3): 771-778.

Chaparro, L., Terradas, J., 2009. Ecological services of urban forest in Barcelona. Institut Municipal de Parcs i Jardins Ajuntament de Barcelona, Àrea de Medi Ambient.

Churkina, G., Running, S.W., 1998. Contrasting climatic controls on the estimated productivity of global terrestrial biomes. Ecosystems, 1(2): 206-215. DOI:https://doi.org/10.1007/s100219900016

Ciais, P., Reichstein, M., Viovy, N., Granier, A., 2005. Europe-wide reduction in primary productivity caused by the heat and drought in 2003. Nature, 437(7058): 529. DOI:https://doi.org/10.1038/nature03972

Comeau, P.G., Kimmins, J.P., 1989. Above-and below-ground biomass and production of lodgepole pine on sites with differing soil moisture regimes. Canadian Journal of Forest Research, 19(4): 447-454.

Cook, E.A., 2007. Green site design: strategies for storm water management. Journal of Green Building, 2(4): 46-56.

Costanza, R., d‟Arge, R., de Groot, R., Farber, S., Grasso, M., Hannon, B., Limburg, K., Naeem, S., O‟Neill, R., V,, Paruelo, J., Raskins, R., Sutton, P., den Belt, M.V., 1997. The value of the world's ecosystem services and natural capital.

Coutts, C., Hahn, M., 2015. Green infrastructure, ecosystem services, and human health. International journal of environmental research and public health, 12(8): 9768-9798.
De Sousa, M.R., Montalto, F.A., Gurian, P., 2016a. Evaluating Green Infrastructure Stormwater Capture Performance under Extreme Precipitation. Journal of Extreme Events, 3(02): 1650006.
De Sousa, M.R., Montalto, F.A., Palmer, M.I., 2016b. Potential climate change impacts on green infrastructure vegetation. Urban Forestry & Urban Greening, 20: 128-139. DOI:https://doi.org/10.1016/j.ufug.2016.08.014
DiBlasi, C.J., Li, H., Davis, A.P., Ghosh, U., 2009. Removal and fate of polycyclic aromatic hydrocarbon pollutants in an urban stormwater bioretention facility. Environmental Science & Technology, 43(2): 494-502.
DiGiovanni, K., Montalto, F., Gaffin, S., 2018. A comparative analysis of micrometeorological determinants of evapotranspiration rates within a heterogeneous urban environment. J. Hydrol., 562: 223-243. DOI:https://doi.org/10.1016/j.jhydrol.2018.04.067
DiGiovanni, K., Montalto, F., Gaffin, S., Rosenzweig, C., 2012. Applicability of classical predictive equations for the estimation of evapotranspiration from urban green spaces: green roof results. J. Hydrol. Eng., 18(1): 99-107. DOI:https://doi.org/10.1061/(ASCE)HE.1943-5584.0000572
DiGiovanni, K.A., 2013. Evapotranspiration from urban green spaces in a Northeast United States City: doctoral dissertation., Drexel University, Philadelphia, PA.
Dorigo, W., Gruber, A., De Jeu, R., Wagner, W., Stacke, T., Loew, A., Albergel, C., Brocca, L., Chung, D., Parinussa, R., 2015. Evaluation of the ESA CCI soil moisture product using ground-based observations. Remote Sensing of Environment, 162: 380-395.
Eisenman, T.S., Churkina, G., Jariwala, S.P., Kumar, P., Lovasi, G.S., Pataki, D.E., Weinberger, K.R., Whitlow, T.H., 2019. Urban trees, air quality, and asthma: An interdisciplinary review. Landscape and urban planning, 187: 47-59.
Escobedo, F.J., Giannico, V., Jim, C.Y., Sanesi, G., Lafortezza, R., 2019. Urban forests, ecosystem services, green infrastructure and nature-based solutions: Nexus or evolving metaphors? Urban forestry & urban greening, 37: 3-12.
Famiglietti, J.S., Ryu, D., Berg, A.A., Rodell, M., Jackson, T.J., 2008. Field observations of soil moisture variability across scales. Water Resour. Res., 44(1).
Galmés, J., Medrano, H., Flexas, J., 2007a. Photosynthetic limitations in response to water stress and recovery in Mediterranean plants with different growth forms. New Phytologist, 175(1): 81-93.
Galmés, J., Ribas-Carbó, M., Medrano, H., Flexas, J., 2007b. Response of leaf respiration to water stress in Mediterranean species with different growth forms. Journal of Arid Environments, 68(2): 206-222.
Gómez-Baggethun, E., Barton, D.N., 2013. Classifying and valuing ecosystem services for urban planning. Ecological economics, 86: 235-245.
Groffman, P.M., Tiedje, J.M., 1989. Denitrification in north temperate forest soils: relationships between denitrification and environmental factors at the landscape scale. Soil Biology and Biochemistry, 21(5): 621-626.

Guo, Q., Hu, Z.-m., Li, S.-g., Yu, G.-r., Sun, X.-m., Li, L.-h., Liang, N.-s., Bai, W.-m., 2016. Exogenous N addition enhances the responses of gross primary productivity to individual precipitation events in a temperate grassland. Scientific reports, 6.

Hartig, T., Evans, G.W., Jamner, L.D., Davis, D.S., Gärling, T., 2003. Tracking restoration in natural and urban field settings. Journal of environmental psychology, 23(2): 109-123.

Hosmer, D.W., Lemeshow, S., Sturdivant, R.X., 2013. Applied logistic regression. John Wiley & Sons, Inc., New York, NY.

Huang, X., Shi, Z., Zhu, H., Zhang, H., Ai, L., Yin, W., 2016. Soil moisture dynamics within soil profiles and associated environmental controls. Catena, 136: 189-196.

Jayasooriya, V., Ng, A., Muthukumaran, S., Perera, B., 2017. Green infrastructure practices for improvement of urban air quality. Urban forestry & urban greening, 21: 34-47.

Jennings, V., Bamkole, O., 2019. The relationship between social cohesion and urban green space: An avenue for health promotion. International journal of environmental research and public health, 16(3): 452.

Jensen, M.E., Allen, R.G., 2016. Evaporation, evapotranspiration, and irrigation water requirements.Task Committee on Revision of Manual 70, 2nd ed. American Society of Civil Engineers, Reston, VA.

Kavehei, E., Jenkins, G., Adame, M., Lemckert, C., 2018. Carbon sequestration potential for mitigating the carbon footprint of green stormwater infrastructure. Renewable and Sustainable Energy Reviews, 94: 1179-1191.

Kavehei, E., Jenkins, G., Lemckert, C., Adame, M., 2019. Carbon stocks and sequestration of stormwater bioretention/biofiltration basins. Ecological Engineering, 138: 227-236.

Kazemi, F., Beecham, S., Gibbs, J., 2009. Streetscale bioretention basins in Melbourne and their effect on local biodiversity. Ecological Engineering, 35(10): 1454-1465.

Kazemi, F., Beecham, S., Gibbs, J., 2011. Streetscape biodiversity and the role of bioretention swales in an Australian urban environment. Landscape and Urban Planning, 101(2): 139-148.

Korres, W., Koyama, C., Fiener, P., Schneider, K., 2010. Analysis of surface soil moisture patterns in agricultural landscapes using Empirical Orthogonal Functions. Hydrology and Earth System Sciences, 14(5): 751-764.

Korres, W., Reichenau, T., Fiener, P., Koyama, C., Bogena, H., Cornelissen, T., Baatz, R., Herbst, M., Diekkrüger, B., Vereecken, H., 2015. Spatio-temporal soil moisture patterns–A meta-analysis using plot to catchment scale data. J. Hydrol., 520: 326-341.

Korres, W., Reichenau, T., Schneider, K., 2013. Patterns and scaling properties of surface soil moisture in an agricultural landscape: An ecohydrological modeling study. J. Hydrol., 498: 89-102.

Koyama, C.N., Korres, W., Fiener, P., Schneider, K., 2010. Variability of surface soil moisture observed from multitemporal C-band Synthetic Aperture Radar and field data. Vadose Zone Journal, 9(4): 1014-1024.

Kurc, S.A., Small, E.E., 2007. Soil moisture variations and ecosystem - scale fluxes of water and carbon in semiarid grassland and shrubland. Water Resour. Res., 43(6).

LeFevre, G.H., Paus, K.H., Natarajan, P., Gulliver, J.S., Novak, P.J., Hozalski, R.M., 2015. Review of dissolved pollutants in urban storm water and their removal and fate in bioretention cells. Journal of Environmental Engineering, 141(1): 04014050.

Liquete, C., Kleeschulte, S., Dige, G., Maes, J., Grizzetti, B., Olah, B., Zulian, G., 2015. Mapping green infrastructure based on ecosystem services and ecological networks: A Pan-European case study. Environmental Science & Policy, 54: 268-280.

Litschke, T., Kuttler, W., 2008. On the reduction of urban particle concentration by vegetation–a review. Meteorologische Zeitschrift, 17(3): 229-240.

Lyytimäki, J., Petersen, L.K., Normander, B., Bezák, P., 2008. Nature as a nuisance? Ecosystem services and disservices to urban lifestyle. Environmental Sciences, 5(3): 161-172.

Lyytimäki, J., Sipilä, M., 2009. Hopping on one leg–The challenge of ecosystem disservices for urban green management. Urban Forestry & Urban Greening, 8(4): 309-315.

Maag, M., Vinther, F.P., 1996. Nitrous oxide emission by nitrification and denitrification in different soil types and at different soil moisture contents and temperatures. Applied Soil Ecology, 4(1): 5-14.

Maes, J., Paracchini, M.L., Zulian, G., 2011. A European assessment of the provision of ecosystem services. Towards and atlas of ecosystem services. Ispra: Joint Research Centre, IES.

Mahmoud, A., Alam, T., Rahman, M.Y.A., Sanchez, A., Guerrero, J., Jones, K.D., 2019. Evaluation of field-scale stormwater bioretention structure flow and pollutant load reductions in a semi-arid coastal climate. Ecological Engineering: X, 1: 100007.

MEA, 2005. Millennium ecosystem assessment Ecosystems and human wellbeing: a framework for assessment Washington, DC: Island Press.

Miller, S.M., Montalto, F.A., 2019. Stakeholder perceptions of the ecosystem services provided by Green Infrastructure in New York City. Ecosystem Services, 37: 100928.

Nemani, R.R., Keeling, C.D., Hashimoto, H., Jolly, W.M., Piper, S.C., Tucker, C.J., Myneni, R.B., Running, S.W., 2003. Climate-driven increases in global terrestrial net primary production from 1982 to 1999. science, 300(5625): 1560-1563. DOI:https://doi.org/10.1126/science.1082750

Nowak, D.J., Crane, D.E., 2002. Carbon storage and sequestration by urban trees in the USA. Environmental pollution, 116(3): 381-389.

NPCC, 2013. Climate risk information 2013: observations, climate change projections, and maps, Retrieved from: http://www.nyc.gov/html/planyc2030/downloads/pdf/npcc_climate_risk_information_2013_report.pdf.

Odum, W.E., Odum, E.P., Odum, H.T., 1995. Nature's pulsing paradigm. Estuaries, 18(4): 547.

Pastor, J., Post, W., 1986. Influence of climate, soil moisture, and succession on forest carbon and nitrogen cycles. Biogeochemistry, 2(1): 3-27.

Peng, C.-Y.J., Lee, K.L., Ingersoll, G.M., 2002. An introduction to logistic regression analysis and reporting. The journal of educational research, 96(1): 3-14.

Penna, D., Brocca, L., Borga, M., Dalla Fontana, G., 2013. Soil moisture temporal stability at different depths on two alpine hillslopes during wet and dry periods. J. Hydrol., 477: 55-71.

Petropoulos, G.P., 2013. Remote sensing of energy fluxes and soil moisture content. CRC Press, Boca Raton, FL.

Pihlatie, M., Syväsalo, E., Simojoki, A., Esala, M., Regina, K., 2004. Contribution of nitrification and denitrification to N 2 O production in peat, clay and loamy sand soils under different soil moisture conditions. Nutrient Cycling in Agroecosystems, 70(2): 135-141.

Pinheiro, C., Chaves, M., 2010. Photosynthesis and drought: can we make metabolic connections from available data? Journal of experimental botany, 62(3): 869-882.

Pugh, T.A., MacKenzie, A.R., Whyatt, J.D., Hewitt, C.N., 2012. Effectiveness of green infrastructure for improvement of air quality in urban street canyons. Environmental science & technology, 46(14): 7692-7699.

R Core Team, 2016. R: A language and environment for statistical computing. . R Foundation for Statistical Computing, Vienna, Austria. Available from: https://www.R-project.org/.

Rai, A., Minsker, B., Sullivan, W., Band, L., 2019. A novel computational green infrastructure design framework for hydrologic and human benefits. Environmental Modelling & Software.

Revelli, R., Porporato, A., 2018. Ecohydrological model for the quantification of ecosystem services provided by urban street trees. Urban Ecosystems, 21(3): 489-504.

Rodriguez‐Iturbe, I., 2000. Ecohydrology: A hydrologic perspective of climate‐soil‐vegetation dynamies. Water Resour. Res., 36(1): 3-9.

Rosenbaum, U., Bogena, H., Herbst, M., Huisman, J., Peterson, T., Weuthen, A., Western, A., Vereecken, H., 2012. Seasonal and event dynamics of spatial soil moisture patterns at the small catchment scale. Water Resour. Res., 48(10).

RStudio Team, 2016. RStudio: Integrated Development for R. RStudio Inc., Boston, MA. Available from: http://www.rstudio.com/.

Shrestha, P., Hurley, S.E., Wemple, B.C., 2018. Effects of different soil media, vegetation, and hydrologic treatments on nutrient and sediment removal in roadside bioretention systems. Ecological Engineering, 112: 116-131.

Smalls-Mantey, L.A., 2017. The Potential Role of Green Infrastructure in the Mitigation of the Urban Heat Island

Susca, T., Gaffin, S.R., Dell'Osso, G., 2011. Positive effects of vegetation: Urban heat island and green roofs. Environmental pollution, 159(8-9): 2119-2126.

Taleghani, M., 2018. Outdoor thermal comfort by different heat mitigation strategies-A review. Renewable and Sustainable Energy Reviews, 81: 2011-2018.

Van Renterghem, T., Botteldooren, D., 2011. In-situ measurements of sound propagating over extensive green roofs. Build. Environ., 46(3): 729-738.

Vereecken, H., Huisman, J., Pachepsky, Y., Montzka, C., Van Der Kruk, J., Bogena, H., Weihermüller, L., Herbst, M., Martinez, G., Vanderborght, J., 2014. On the spatio-temporal dynamics of soil moisture at the field scale. J. Hydrol., 516: 76-96.

Western, A.W., Grayson, R.B., Green, T.R., 1999. The Tarrawarra project: high resolution spatial measurement, modelling and analysis of soil moisture and hydrological response. Hydrological processes, 13(5): 633-652.

Williams, C.A., Albertson, J.D., 2004. Soil moisture controls on canopy‐scale water and carbon fluxes in an African savanna. Water Resour. Res., 40(9).

Winston, R.J., Dorsey, J.D., Hunt, W.F., 2016. Quantifying volume reduction and peak flow mitigation for three bioretention cells in clay soils in northeast Ohio. Sci. Total Environ., 553: 83-95.

WWAP (United Nations World Water Assessment Programme), 2018. The United Nations World Water Development Report 2018: Nature-Based Solutions for Water. UNESCO Paris.

Xu, Z., Zhou, G., Shimizu, H., 2010. Plant responses to drought and rewatering. Plant signaling & behavior, 5(6): 649-654.

Yao, S., Zhao, C., Zhang, T., Liu, X., 2013. Response of the soil water content of mobile dunes to precipitation patterns in Inner Mongolia, northern China. Journal of arid environments, 97: 92-98.

Yu, Z., Miller, S., Montalto, F., Lall, U., 2018. The bridge between precipitation and temperature – Pressure Change Events: Modeling future non-stationary precipitation. J. Hydrol., 562: 346-357. DOI:10.1016/j.jhydrol.2018.05.014

Yu, Z., Miller, S., Montalto, F., Lall, U., 2019. Development of a Non-Parametric Stationary Synthetic Rainfall Generator for Use in Hourly Water Resource Simulations. Water, 11(8). DOI:10.3390/w11081728